Atmos. Chem. Phys. Discuss., doi:10.5194/acp-2016-932, 2016
Manuscript under review for journal Atmos. Chem. Phys.
Published: 5 December 2016

Atmospheric Chemistry and Physics Discussions

Biomass burning at Cape Grim: exploring photochemistry using multi-scale modelling

Sarah J. Lawson[1], Martin Cope[1], Sunhee Lee[1], Ian E. Galbally[1], Zoran Ristovski[2] and Melita D. Keywood[1]

[1] Commonwealth Scientific and Industrial Research Organisation, Climate Science Centre, Aspendale, Australia

[2] International Laboratory for Air Quality & Health, Queensland University of Technology, Brisbane, Australia

Correspondence to: S. J. Lawson (sarah.lawson@csiro.au)

Abstract

We have tested the ability of high resolution chemical transport modelling (CTM) to reproduce biomass burning (BB) plume strikes observed at Cape Grim in Tasmania Australia from the Robbins Island fire. The model has also been used to explore the contribution of near-field BB emissions and background sources to ozone (O_3) under conditions of complex meteorology. Using atmospheric observations, we have tested model sensitivity to meteorology, BB emission factors (EF) corresponding to low, medium and high modified combustion efficiency (MCE) and spatial variability. The use of two different meteorological models varied the first (BB1) plume strike time by up to 15 hours, and duration of impact between 12 and 36 hours, while the second plume strike (BB2) was simulated well using both meteorological models. Meteorology also had a large impact on simulated O_3, with one model (TAPM-CTM) simulating 4 periods of O_3 enhancement, while the other model (CCAM) simulating only one period. Varying the BB EFs which in turn varied the non methanic-organic compound (NMOC) / oxides of nitrogen (NO_x) ratio had a strongly non-linear impact on O_3 concentration, with either destruction or production of O_3 predicted in different simulations. As shown in the previous work (Lawson et al., 2015), minor rainfall events have the potential to significantly alter EF due to changes in combustion processes. Models which assume fixed EF for O_3 precursor species in an environment with temporally or spatially variable EF may be unable to simulate the behaviour of important species such as O_3.

Atmos. Chem. Phys. Discuss., doi:10.5194/acp-2016-932, 2016
Manuscript under review for journal Atmos. Chem. Phys.
Published: 5 December 2016

Atmospheric Chemistry and Physics Discussions

TAPM-CTM is used to explore the contribution of the Robbins Island fire to the observed O_3 enhancements during BB1 and BB2. Overall, the model suggests the dominant source of O_3 observed at Cape Grim was aged urban air (age = 2 days), with a contribution of O_3 formed from local BB emissions. The model indicates that in an area surrounding Cape Grim, between 25 - 43% of O_3 enhancement during BB1 was formed from BB emissions while the fire led to a net depletion in O_3 during BB2.

This work shows the importance of assessing model sensitivity to meteorology and EF, and the large impact these variables can have in particular on simulated destruction or production of O_3. This work also demonstrates how a model can be used to elucidate the degree of contribution from different sources to atmospheric composition, where this is difficult using observations alone.

1 Introduction

Biomass burning (BB) makes a major global contribution to atmospheric trace gases and particles with ramifications for human health, air quality and climate. Directly emitted species include carbon monoxide (CO), carbon dioxide (CO_2), oxides of nitrogen (NO_x), primary organic aerosol (POA), non-methanic organic compounds (NMOC) and black carbon (BC), while chemical transformations occurring in the plume over time lead to formation of secondary species such as O_3, oxygenated NMOC and secondary aerosol. Depending on a number of factors, including magnitude and duration of fire, plume rise and meteorology, the impact of BB plumes from a fire may be local, regional or global.

BB plumes from wildfires, prescribed burning, agricultural and trash burning can have a major impact on air quality in both urban and rural centres (Keywood et al., 2015; Luhar et al., 2008; Reisen et al., 2011; Emmons et al., 2010; Yokelson et al., 2011) and regional scale climate impacts (Andreae et al., 2002; Keywood et al., 2011b; Artaxo et al., 2013; Anderson et al., 2016). In Australia, BB from wild and prescibed fires impacts air quality in both rural and urban areas (Keywood et al., 2015; Reisen et al., 2011; Luhar et al., 2008; Keywood et al., 2011a) as well as indoor air quality (Reisen et al., 2011). More generally, as human population density increases, and as wildfires become more frequent (Flannigan et al., 2009; Keywood et al., 2011b), assessing the impact of BB on air quality and human health becomes more urgent (Keywood et al., 2011b; Reisen et al., 2015). In particular, particles emitted from BB frequently lead to exceedances of air quality standards, and exposure to BB particles has been linked to

Atmos. Chem. Phys. Discuss., doi:10.5194/acp-2016-932, 2016
Manuscript under review for journal Atmos. Chem. Phys.
Published: 5 December 2016

Atmospheric Chemistry and Physics Discussions

poor health outcomes including respiratory effects, cardiovascular disease and mortality (Reisen et al., 2015; Reid et al., 2016; Dennekamp et al., 2015). There is also increasing evidence that mixing of BB emissions with urban emissions results in enhanced photochemistry and production of secondary pollutants such as secondary aerosol and O_3 (Jaffe and Wigder, 2012; Akagi et al., 2013; Hecobian et al., 2012), which may result in more significant health impacts than exposure to unmixed BB or urban emissions.

To be able to accurately predict and assess the impact of BB on human health, air quality and climate, models must be able to realistically simulate the chemical and microphysical processes that occur in a plume as well as plume transport and dispersion. In the case of BB plumes close to an urban centre or other sensitive receptor, models can be used to mitigate risks on community by forecasting where and when a BB plume will impact, the concentrations of toxic trace gases and particles in the plume, and potential impact of the BB plume mixing with other sources. Models also allow investigation of the contributions from BB and other sources on observed air quality when multiple sources are contributing. Understanding the relative importance of different sources is required when formulating policy decisions to improve air quality.

Lagrangian parcel models are often used to investigate photochemical transformations in BB plumes as they are transported and diluted downwind (Jost et al., 2003; Trentmann et al., 2005; Mason et al., 2006; Alvarado and Prinn, 2009; Alvarado et al., 2015) while three-dimensional (3D) Eulerian grid models have been used to investigate transport and dispersion of plumes, plume age, as well as contributions from different sources. 3D Eulerian grid models vary from fine spatial resolution on order of kms (Luhar et al., 2008; Keywood et al., 2015; Alvarado et al., 2009; Lei et al., 2013) to a resolution of up to hundreds of km in global models (Arnold et al., 2015; Parrington et al., 2012).

Broadly speaking, models used for simulating BB plumes comprise a) description of the emissions source b) a determination of plume rise c) treatment of the vertical transport and dispersion and d) a mechanism for simulating chemical transformations in the plume (Goodrick et al., 2013). There are challenges associated with accurately representing each of these components in BB modelling. The description of emissions source includes a spatial and temporal description of the area burnt, the fuel load, combustion completeness, and trace gas and aerosol emission factors per kg of fuel burned. The area burned is often determined by a combination of hotspot and fire scar data, determined from retrievals from satellite (Kaiser et al., 2012; Reid et al., 2009). Cloud cover may lead to difficulties in obtaining area burnt data,

Atmos. Chem. Phys. Discuss., doi:10.5194/acp-2016-932, 2016
Manuscript under review for journal Atmos. Chem. Phys.
Published: 5 December 2016

Atmospheric Chemistry and Physics Discussions

while scars from small fires may be difficult to discern against complex terrain, and low intensity fires may not correspond with a detectable hotspot (Meyer et al., 2008). Emission factors are determined experimentally either by field or laboratory measurements, and are typically grouped by biome type. In some regions, such as SE Australia, biomes have been sparsely characterised (Lawson et al., 2015). Furthermore, models use biome–averaged EF which do not account for complex intra-biome variation in EF as a result of temporal and spatial differences in environmental variables. This includes factors such as impact of vegetation structure, monthly average monthly rainfall (van Leeuwen and van der Werf, 2011) and the influence of short term rainfall events (Lawson et al., 2015). Finally, the very complex mixture of trace gases and aerosols in BB plumes creates analytical challenges in quantifying EF, especially for semi and low volatility organics which are challenging to measure and identify but contribute significantly to secondary aerosol formation and photochemistry within the plume (Alvarado and Prinn, 2009; Alvarado et al., 2015; Ortega et al., 2013).

Plume rise is a description of how high the buoyant smoke plume rises above the fire, and consequently the initial vertical distribution of trace gases and aerosols in the plume (Freitas et al., 2007). This is still a large area of uncertainty in BB models, with a generalised plume rise approach typically used which may include either homogenous mixing, prescribed fractions of emissions distributed according to mixing height, use of parametisations, and finally plume rise calculated according to atmospheric dynamics. A key driver of this uncertainty is the complexity of fire behaviour resulting in high spatial and temporal variability of pollutant and heat release, which drives variability in plume rise behaviour, such as multiple updraft cores (Goodrick et al., 2013).

Transport and dilution in models is driven by meteorology, particularly wind speed and direction, wind shear and atmospheric stability. Meteorology has a large impact on the ability of models to simulate the timing and magnitude and even composition of BB plume impacts in both local and regional scale models (Lei et al., 2013; Luhar et al., 2008; Arnold et al., 2015). For example, too-high wind speeds can lead to modelled pollutant levels which are lower than observed (e.g. Lei et al., (2013)) while small deviations in wind direction lead to large concentration differences between modelled and observed, particularly when modelling emissions of multiple spatially diverse fires (Luhar et al., 2008). Dilution of BB emissions in large grid boxes in global models may also lead to discrepancies between modelled and observed NO_x, O_3 and aerosols (Alvarado et al., 2009).

Atmos. Chem. Phys. Discuss., doi:10.5194/acp-2016-932, 2016
Manuscript under review for journal Atmos. Chem. Phys.
Published: 5 December 2016

Finally, models use a variety of gas-phase and aerosol-phase physical and chemical schemes, which vary in their ability to accurately represent chemical transformations, including formation of O_3 and organic aerosol (Alvarado and Prinn, 2009; Alvarado et al., 2015). Validating and constraining chemical transformations in models requires high quality, high time resolution BB observations of a wide range of trace gas and aerosol species, including important but infrequently measured species such as OH and semi volatile and low volatility NMOC. Field observations, whilst often temporally and spatially scarce, are particularly valuable because the processes and products of BB plume processing are dependent on long range transport, cloud processing, varying meteorological conditions and heterogeneous reactions.

Sensitivity studies have allowed the influence of different model components (emissions, plume rise, transport, chemistry) on model output to be investigated. Such studies are particularly important in formation of secondary species such as O_3 which have a non-linear relationship with emissions. Studies have found that modelled O_3 concentration from BB emissions is highly dependant on a range of factors including a) meteorology (plume transport and dispersion) in global (Arnold et al., 2015) and high resolution (Lei et al., 2013) Eulerian grid models, b) absolute emissions/biomass burned (Pacifico et al., 2015; Parrington et al., 2012), c) model grid size resulting in different degrees of plume dilution (Alvarado et al., 2009), and oxidative photochemical reaction mechanisms in Lagrangian parcel models (Mason et al., 2006).

In this work we test the ability of a high resolution 3D Eulerian grid chemical transport model to reproduce BB plume observations of the Robbins Island fire reported in Lawson et al., (2015) with a focus on CO, BC and O_3. The fire and fixed observation site (Cape Grim) were only 20km apart, and so simulation of the plume strikes is a stringent test of the model's ability to reproduce windspeed and direction. We undertake sensitivity studies using varying emission factors associated with a low, medium and high Modified Combustion Efficiency (MCE), which in turn changes the NMOC / NO_x ratio, in contrast to other sensitivity studies which typically vary emissions linearly. We also test the model sensitivity to meteorology by utilising two different meteorological models. Plume rise and chemical mechanism are held constant. Finally, we use the model to separate the contribution of the Robbins Island fire emissions and urban emissions to the observed O_3 enhancements at Cape Grim reported in Lawson et al., (2015), and use the model to determine the age of the O_3-enhanced air parcels.

Atmos. Chem. Phys. Discuss., doi:10.5194/acp-2016-932, 2016
Manuscript under review for journal Atmos. Chem. Phys.
Published: 5 December 2016

Atmospheric Chemistry and Physics Discussions

2 Methods

2.1 Fire and measurement details

Details of the fire and measurements are given in Lawson et al (2015). Briefly, biomass burning (BB) plumes were measured at the Cape Grim Baseline Air Pollution Station during the 2006 Precursors to Particles campaign, when emissions from a fire on nearby Robbins Island impacted the station. Fire burned through native heathland and pasture grass on Robbins Island some 20 km to the east of Cape Grim for two weeks in February 2006. Plume strikes occurred on two occasions when an easterly wind advected the BB plume directly to Cape Grim. The first plume strike (BB1) occured from 02:00 – 06:00 (Australian Eastern Standard Time - AEST) on the 16th February while the second, more prolonged plume strike (BB2) occurred from 23:00 on 23rd February to 05:00 on the 25th February. In northerly winds, urban air from Melbourne city (population 4.2 million) ~300 km away is transported to Cape Grim. Further details can be found in Lawson et al., (2015).

A wide variety of trace gas and aerosol measurements were made during the fire event (Lawson et al., 2015). In this work, measurements of black carbon (BC), carbon monoxide (CO) and ozone (O_3) are compared with model output.

2.2 Chemical transport models

Simulations were undertaken with a chemical transport model (CTM), coupled offline with two meteorological models (see below). The CTM is a three-dimensional Eulerian chemical transport model with the capability of modelling the emission, transport, chemical transformation, wet and dry deposition of a coupled gas and aerosol phase atmospheric system. The CTM was initially developed for air quality forecasting (Cope et al., 2004) and has had extensive use with shipping emission simulations (Broome et al., 2016), urban air quality (Cope et al., 2014; Galbally et al., 2008), biogenic (Emmerson et al., 2016) and biomass burning studies (Keywood et al., 2015; Meyer et al., 2008; Luhar et al., 2008).

The chemical transformation of gas-phase species was modelled using an extended version of the Carbon Bond 5 mechanism (Sarwar et al., 2008) with updated toluene chemistry (Sarwar et al., 2011). The mechanism also includes the gas phase precursors for secondary (gas and aqueous phase) inorganic and organic aerosols. Secondary inorganic aerosols are assumed to exist in thermodynamic equilibrium with gas phase precursors and were modelled using the ISORROPIA-II model (Fountoukis and Nenes, 2007). Secondary organic aerosol (SOA) was

Atmos. Chem. Phys. Discuss., doi:10.5194/acp-2016-932, 2016
Manuscript under review for journal Atmos. Chem. Phys.
Published: 5 December 2016

modelled using the Volatility Basis Set (VBS) approach (Donahue et al., 2006). The VBS configuration is similar to that described in Tsimpidi et al., (2010). The production of S-VI in cloud water was modelled using the approach described in Seinfeld and Pandis (1998). The boundary concentrations in the model for different wind directions were informed by Cape Grim observations of atmospheric constituents during non BB periods (Lawson et al., 2015). In this work the modelled elemental carbon (EC) output was considered equivalent to the BC measured with aethalometer at Cape Grim.

Horizontal diffusion is simulated according to equations detailed in Cope et al (2009) according to principles of Smagorinsky et al., (1963) and Hess (1989). Vertical diffusion is simulated according to equations detailed in Cope et al., (2009) according to principles of Draxler and Hess (1997). Horizontal and vertical advection uses the approach of Walcek et al., (2000).

2.2.1 Meteorological models

Prognostic meteorological modelling was used for the prediction of meteorological fields including wind velocity, temperature, and water vapour mixing ratio (including clouds), radiation and turbulence. The meteorological fields force key components of the emissions and the chemical transport model. Two meteorological models were used in this work. CSIRO's TAPM (Hurley, 2008b), a limited area, nest-able, three-dimensional Eulerian numerical weather and air quality prediction system, and CSIRO's Conformal Cubic Atmospheric Model (CCAM) a global stretched grid atmospheric simulation model (McGregor, (2015) and references therein). The model was run using five nested computational domains with cell spacings of 20 km, 12 km, 3 km, 1 km and 400 m (Figure 1). This multi-scale configuration was required in order to capture a) large scale processes such as windblown dust, sea salt aerosol and ambient fires; b) transport of the Melbourne urban plume to Cape Grim; c) transport of the Robbin's Island smoke plume between the point of emission and Cape Grim.

In this work the CTM coupled with CCAM meteorological model is referred to as CTM-CCAM, while the CTM coupled with the TAPM meteorological model is referred to as TAPM-CTM.

2.2.2 Emission inventories

Anthropogenic emissions

Anthropogenic emissions for Victoria were based on the work of Delaney et al (2011). No anthropogenic emissions were included for Tasmania. The north-west section of Tasmania has

Atmos. Chem. Phys. Discuss., doi:10.5194/acp-2016-932, 2016
Manuscript under review for journal Atmos. Chem. Phys.
Published: 5 December 2016

limited habitation and is mainly farmland, and so the influence of Tasmanian anthropogenic emissions on Cape Grim are expected to be negligible.

Natural and Biogenic emissions

The modelling framework includes methodologies for estimating emissions of sea salt aerosol (Gong, 2003) emissions of windblown dust (Lu and Shao, 1999); gaseous and aerosol emissions from managed and unmanaged wild fires (Meyer et al., 2008); emissions of NMOC from vegetation (Azzi et al., 2012) and emissions of nitric oxide and ammonia from vegetation and soils. Emissions from all but the wildfires are calculated inline in the CTM at each time step using the current meteorological fields. There were no other major fires burning in Victoria and Tasmania during the study period.

Robbins Island fire emissions

An image of the fire scar on Robbins Island at the end of February 2006 was the only information available about the area burned and there was no detailed information available about the direction of fire spread. The fire burnt over the two week period, and the area burnt was subdivided into hourly amounts burnt using a normalised version of the Macarthur Fire Danger Index. Therefore area burnt was divided up into 250m grids, and the model assumed that an equal proportion of each grid burned simultaneously over the two week period. The fuel density used was estimated to be 18.7 t C ha^{-1}, based on mean mass loads of coarse and fine fuels taken from the biogeochemical production model (VAST 1.2, Barrett 2002) and converted into carbon mass (Meyer et al., 2008).

The hourly diurnal emissions of all gases and particles from the fire were calculated using the Macarthur Fire Danger Index (FDI) (Meyer et al., 2008) in which the presence of strong winds will result in faster fire spread and enhanced emissions, compared to periods of lower wind speeds (Figure 2). The effect of wind speed on the fire behaviour and emissions in particularly important during the second BB event in which the winds ranged from 10 to15 m s^{-1}.

Savanna category EF were used as base case EFs in this work from Andreae and Merlet (2001). Three different sets of fire emission factors, corresponding to low, medium and high modified combustion efficiency (MCE) were used to test the sensitivity of the model, where MCE = $\Delta CO_2 / \Delta CO + \Delta CO_2$ (Ferek et al., 1998). We used reported EF of CO and CO_2 from temperate forests (Akagi et al., 2011), to calculate a typical range of MCEs for temperate fires, including an average (best estimate) of 0.92, a lower (0.89) and upper estimate (0.95). Fires with MCEs of approximately 0.90 consume biomass with approximately equal amounts of smouldering

Atmos. Chem. Phys. Discuss., doi:10.5194/acp-2016-932, 2016
Manuscript under review for journal Atmos. Chem. Phys.
Published: 5 December 2016

and flaming, while MCEs of 0.99 indicate complete flaming combustion (Akagi et al., 2011). Therefore the calculated range of MCEs (0.89 - 0.95) correspond to fires in which both smouldering and flaming is occurring, with a tendency for more flaming combustion in the upper estimate (0.95) compared to a tendency of more smouldering in the lower estimate (0.89). The CO EF for lower, best estimate and upper MCE were taken as minimum, mean and maximum EF for temperate forests summarised by Akagi et al., (2011). For all other species, the savannah fuel EF (Andreae and Merlet, 2001) were adjusted according to published relationships between MCE and EF (Meyer et al., 2012; Yokelson et al., 2007; Yokelson et al., 2003; Yokelson et al., 2011). For example to adjust from the savannah EF (corresponding to an MCE of 0.94) to our temperate 'best estimate' EF (corresponding to MCE of 0.92), all NMOC EF's were increased by a factor of 1.3, as an approximate response based on relationships between MCE and EF for CH_4 (Meyer et al., 2012), methanol (Yokelson et al., 2007), HCN and formaldehyde (Yokelson et al., 2003). The savannah BC EF (Andreae and Merlet, 2001) was reduced by 30%, and the OC EF was increased by 20%, based on the relationship reported in Yokelson et al., (2011), in which smouldering results in lower EC and higher OC emission. The Andreae and Merlet (2001) savannah NO EF from was reduced by 30% according to the relationship in (Yokelson et al., 2007). Table 1 shows emission factors which correspond to the three MCEs.

We recognise calculating EF in this way is approximate, however the purpose of including a range of EF was to explore the model sensitivity to EF. EFs were calculated for the Robbins Island fire for several species (Lawson et al., 2015), but these EF are only available for a subset of species required by the CB05 chemical mechanism and so EF currently used in the model for Savannah fires were adjusted as described above to better reflect the likely range of EF expected in temperate fires. The adjustment of the Andreae and Merlet (2001) Savannah EF to a lower MCE (0.89) resulted in good (± 20%) agreement with the calculated EF for CO, BC and several NMOC from Lawson et al., (2015), in which the MCE was calculated as 0.88. This provides confidence in using published relationships between MCE and EF to estimate EF in this work.

Plume rise

The chemical transport model calculates plume rise from buoyant sources and/or sources with appreciable vertical momentum within the computational time step loop. In the case of industrial sources (such as power stations) plume rise is calculated by numerically integrating state equations for the fluxes of moment and buoyancy according to the approach used in

Atmos. Chem. Phys. Discuss., doi:10.5194/acp-2016-932, 2016
Manuscript under review for journal Atmos. Chem. Phys.
Published: 5 December 2016

TAPM (Hurley, 2008a). In the case of landscape fires, there are a hierarchy of approaches which can be used (Paugam et al., 2016), including rule-of-thumb, simple empirical approaches, and deterministic models varying in complexity from analytic solutions to cloud resolving numerical models. The Robbin's Island fire was a relatively low energy burn (Lawson et al., 2015), and as noted by Paugam et al., (2016) the smoke from such fires is largely contained within the planetary boundary layer (PBL). Given that ground-based images of the Robbin's Island smoke plume support this hypothesis, in this work we adopted a simple approach of mixing the emitted smoke uniformly into the model layers contained within the PBL.The plume was well mixed between the minimum of the PBL height and 200m above the ground, with the latter included to account for some vertical mixing of the buoyant smoke plume even under conditions of very low PBL height. The high wind speeds particularly during the second BB event, also suggest that the plume was not likely to be sufficiently buoyant to penetrate the PBL.

3 Results and Discussion

3.1 Modelling Sensitivity Study

The ability of the model to reproduce the two plume strikes (BB1 and BB2, described in Lawson et al (2015)) was tested. The sensitivity of the model to meteorology, emission factors and spatial variability was also investigated and is discussed below. Observation and model data shown are hourly averages. Table 2 summarises main findings of the model sensitivity study. A MODIS Truecolour Aqua image of the Robbins Island fire plume is shown in Figure 3 from the 23 February 2006, with the modelled plume during the same period.

3.1.1 Sensitivity of model to meteorology

Before investigating impact of different meteorology models on concentrations of chemical species, modelled wind speed and direction were compared with observations at Cape Grim. Briefly, throughout the study period wind direction simulated by TAPM and CCAM agreed very well with observed wind direction at Cape Grim, with the exception of some differences in timing between observed and modelled wind direction change from easterly to north north-westerly (discussed below) on the 16th February. Throughout the study period TAPM and CCAM underestimated observed wind speeds by an average of 2.5 m s^{-1} and 1.8 m s^{-1} respectively.

Atmos. Chem. Phys. Discuss., doi:10.5194/acp-2016-932, 2016
Manuscript under review for journal Atmos. Chem. Phys.
Published: 5 December 2016

Primary species- CO and BC

Figure 4 shows a typical output of spatial plots from CCAM-CTM for BB1 with the model output every 12 hours shown. The narrow BB plume is simulated intermittently striking Cape Grim (until 17 Feb 4:00), and then the plume is swept away from Cape Grim after a wind direction change.

The simulated and observed time series concentrations of CO and BC for the two different models (TAPM-CTM and CCAM-CTM) and for 3 different sets of EF (discussed in Section 3.1.2) are shown in Figure 5. TAPM-CTN and CCAM-CTM both reproduce the observed plume strikes (BB1 and BB2). The impact of meteorology on the plume strike timing and duration is discussed below.

Both models overestimate the duration of BB1 and are a few hours out in the timing of the plume strike. TAPM-CTM predicts the timing of BB1 to be about 3 hours later than occurred (BC data) and predicts that BB1 persists for 12 hours (actual duration 5 hours). CCAM-CTM predicts that BB1 occurs 12 hours prior to the observed plume strike and predicts that the plume intermittently sweeps across Cape Grim for up to 36 hours (Figure 4) (5 hours actual). Both models indicate that the plume is narrow and meandering.

In contrast, both models successfully predict the timing and duration of BB2. TAPM-CTM correctly predicts the timing of the first enhancement of BC prior to BB2 (if the first BC enhancement on the 22 Feb at 20:00 is included) and predicts that BB2 persists for 50 hours (actual duration 57 hours). CCAM-CTM correctly predicts the timing and duration of BB2 (57 hours modelled and observed).

The difference between the TAPM and CCAM simulated wind direction is driving these differences. In both BB1 and BB2, the plume strike at Cape Grim occurred just prior to a wind direction change from easterly (fire direction), to north-north westerly. The timing of the wind direction change in the models is therefore crucial to correctly predicting plume strike time and duration. In BB1 CCAM predicts an earlier wind direction change with higher windspeeds which advects the plume directly over Cape Grim while TAPM predicts a later wind change, lower windspeeds and advection of only the edge of the plume over Cape Grim. In BB2, both models predict similar wind speeds and directions, and a direct 'hit' of the plume over the station.

The magnitudes of the BC and CO peaks shown are also influenced by meteorology. Overall, CCAM-CTM predicts higher concentrations of CO and BC in BB1, and TAPM predicts higher

Atmos. Chem. Phys. Discuss., doi:10.5194/acp-2016-932, 2016
Manuscript under review for journal Atmos. Chem. Phys.
Published: 5 December 2016

concentrations in BB2. Assuming a constant EF, peak magnitudes are influenced by several factors including wind direction (directness of plume hit), wind speed (degree of dispersion and rate of fuel combustion, see Section 2.2.2) and PBL height (degree of dilution). In BB1, the larger BC and CO concentrations in CCAM are likely due to the direct advection of the plume over the site compared to only the plume edge in TAPM. In BB2, both CCAM and TAPM predict direct plume strikes, and the higher CO and BC peaks in TAPM are likely due to a lower PBL in TAPM which leads to lower levels of dilution and more concentrated plume.

Secondary species – O_3

Figure 5 e-f shows the simulated and actual O_3 concentration time series for TAPM-CTM and CCAM-CTM for 3 different sets of EF (discussed in Section 3.1.2). The two observed O_3 peaks which followed BB1 and BB2 can clearly be seen in the time series.

Again the simulated meteorology has a major impact on the ability of the model to reproduce the magnitude and timing of the observed O_3 peaks. TAPM reproduces both of the major O_3 peaks observed following BB1 and BB2, with the timing of the first peak within 5 hours of the observed peak and the second within 8 hours of the observed peak. The model also shows 2 additional O_3 peaks about 24 hours prior to the BB1 and BB2 peaks respectively which were not observed at the Cape Grim. The magnitude of these additional peaks shows a strong dependency on the EF suggesting an influence of fire emissions. This is discussed further below and in Section 3.2.1.

Compared to TAPM, CCAM generally shows only minor enhancements of O_3 above background. Both TAPM and CCAM show depletion of O_3 below background levels which was not observed, and this is discussed further in Section 3.1.2.

To summarise, the impact of using two different meteorological models for a primary species such as BC was to vary the modelled time of impact of the BB1 plume strike by up to 15 hours (CCAM -12 and TAPM +3 hours, where actual plume strike time = 0 hours) and to vary the plume duration between 12 and 36 hours (actual duration 5 hours).

For O_3, the use of different meteorological models lead to one model (TAPM) reproducing both observed peaks plus two additional peaks, while the other model (CCAM) captured only one defined O_3 peak over the time series of 2 weeks.

Atmos. Chem. Phys. Discuss., doi:10.5194/acp-2016-932, 2016
Manuscript under review for journal Atmos. Chem. Phys.
Published: 5 December 2016

Atmospheric Chemistry and Physics Discussions

3.1.2 Sensitivity of modelled BB species to Emission Factors

Primary species – CO and BC

Figure 5 a-d shows the simulated and observed concentrations of BC and CO for combustion MCEs of 0.89, 0.92 and 0.95 (see Method Section 2.2.2). Because CO has a negative relationship with MCE, and BC has a positive relationship with MCE, the modelled BC concentrations are highest for model runs using the highest MCE, while the modelled CO concentrations are highest for model runs using the lowest MCE (Figure 5).

Changing the EF from low to high MCE varies the modelled BC concentrations during BB1 and BB2 by a factor of ~3 for BC and a factor of ~2 for CO, and for these primary pollutants this is in proportion to the difference in EF input to the model.

Observed CO and BC peaks were compared in magnitude to peaks simulated using different EF in CCAM-CTM and TAPM-CTM. In TAPM, the simulation with the lowest combustion efficiency EFs (MCE 0.89) gives closest agreement to the CO observations, while the run with the medium combustion efficiency EFs (MCE 0.92) gives best agreement with BC observations. For CCAM, the lowest MCE model run (0.89) provides the best agreement with observations for CO for BB and BB2, while for BC, model runs corresponding to the low MCE 0.89 (BB1) and high MCE 0.95 (BB2) provide the best agreement with observations.

As discussed in Section 3.1.1, the magnitude of the modelled concentration is a function of both the input EF, the wind speed (rate of fuel burning, dispersion) and the mixing height which controls the degree of dilution after plume injection. Hence a good agreement between the magnitude of the model and observed peaks is not necessarily indicative that a suitable set of EF has been used. As discussed previously there is also uncertainty in the derivation of EF as a function of MCE, as these were based on relationships from a small number of studies. However interestingly, in most cases, model simulations with EF corresponding to the low MCE 0.89 appear to best represent the observations, which is in agreement with the calculated MCE of 0.88 for this fire (Lawson et al., 2015).

Secondary species - O_3

For secondary species O_3 (Figure 5e-f), the relationship between EF precursor gases and model output is more complex than for primary species such as CO and BC, because the balance

Atmos. Chem. Phys. Discuss., doi:10.5194/acp-2016-932, 2016
Manuscript under review for journal Atmos. Chem. Phys.
Published: 5 December 2016

between O_3 formation and destruction is dependent on the degree of dilution of the BB emissions and also factors such as the NMOC composition and the NMOC/NO_x ratio.

TAPM-CTM (Figure 5e) reproduces the magnitude of both observed peaks following BB1 and BB2 (BB1 max observed = 33 ppb, modelled = 31 ppb, BB2 max observed = 34 ppb, modelled = 30ppb). Interestingly the magnitude of O_3 for these two peaks is the same for different EF inputs of O_3 precursors from the Robbins Island fire, suggesting that the BB emissions are not responsible for these enhancements. In contrast, the two additional peaks modelled but not seen in the observations are heavily dependent on the input EF. For the first additional peak modelled prior to BB1, all EF runs result in an O_3 peak, with the medium MCE model scenario resulting in highest predicted O_3. For the second additional modelled peak prior to BB2, only the lowest MCE model run results in a net O_3 production, while medium and high MCE runs lead to net O_3 destruction.

This differing response to EF for the TAPM runs suggests the importance of the NO EF on O_3 production in BB plumes. Unfortunately there were no oxides of nitrogen measurements made during the fire to test the model. For the first simulated additional peak prior to BB1, while the medium NO EF (MCE 0.92) resulted in the highest O_3 peak (with corresponding NO of 3.7 ppb, NO_2 4.5 ppb) the lower NO EF in the 0.89 MCE run perhaps indicates insufficient NO was present to drive O_3 production (corresponding NO 0.5 ppb, NO_2 1.5 ppb), which is in line with studies which have shown that BB plumes are generally NO_x limited (Akagi et al., 2013; Jaffe and Wigder, 2012; Wigder et al., 2013). Conversely the highest input NO EF (MCE 0.95) lead to net destruction of O_3 (NO 9 ppb, NO_2 7 ppb), which is due to titration of O_3 with the larger amounts of NO emitted from the fire in these runs as indicated by excess NO (NO/NO_2 ratio > 1) at Cape Grim (where NO has a positive relationship with MCE). For the second additional peak prior to BB2, only the lowest NO EF run (MCE 0.89) resulted in net production of O_3 (NO 1.5 NO_2 2.6)– in the medium and high MCE runs the background O_3 concentration is completely titrated (0 ppb) with NO concentrations of 10 and 20 ppb and NO/NO_2 ratios of 1.3 and 2.6 respectively.

Unlike the simulation, the observations do not show significant reduction of O_3 below background levels. The lower MCE (0.89) TAPM-CTM model simulation predicts no O_3 titration and is in best agreement with the observations. This suggests that EF corresponding to lower MCE (0.89) are most representative of the combustion conditions during the Robbins Island fire, and as stated previously is in agreement with the calculated MCE of 0.88 for BB2 (Lawson et al., 2015). Again however it should be recognised that the absolute concentrations

Atmos. Chem. Phys. Discuss., doi:10.5194/acp-2016-932, 2016
Manuscript under review for journal Atmos. Chem. Phys.
Published: 5 December 2016

of NO in the plume, which determines O_3 production or destruction, are not only driven by EF but also dependent on the degree of dilution, which is driven by meteorology and mixing height.

In contrast, the CCAM-CTM model (Figure 5f) simulations reproduce only the first observed O_3 peak associated with BB1 (modelled = 27 ppb, measured = 34 ppb). This modelled O_3 peak does not show an influence of MCE on O_3 concentration, in agreement with TAPM, again suggesting no influence from fire emissions. The CCAM model runs also show significant titration of O_3 during BB1 and BB2 for the medium and high MCE model runs, with ~24 and ~48 hours of significant O_3 depletion below background concentrations being modelled for each event, which was not observed.

To summarise, the impact of EF on primary species such as BC and CO was that the modelled peak concentrations varied in proportion with the variation in the input EFs, (factor of ~3 BC and ~2 CO). For the secondary species O_3, the EF of precursor gases, particularly NO_x, had a major influence (along with meteorology) on whether the model predicted net production of O_3, or destruction of background O_3, as was particularly evident in TAPM-CTM.

As shown in the previous work (Lawson et al., 2015), minor rainfall events have the potential to significantly alter EF due to changes in combustion processes. This work suggests that varying model EF may have a major impact on whether the model predicts production or destruction of O_3, particularly important at a receptor site in close proximity to the BB emissions. Models which assume a fixed EF for O_3 precursor species in an environment with temporally variable EF may therefore be challenged to correctly predict the behaviour of an important species such as O_3.

Given that TAPM-CTM meteorological model with EF corresponding to the low combustion efficiency (MCE 0.89) provides an overall better representation of the timing and magnitude of both primary and secondary species during the fire, this configuration has been used to further explore the spatial variability in the next section, as well as drivers of O_3 production and plume age in Section 3.2 and 3.3.

3.1.3 Sensitivity of modelled concentrations to spatial variability

The near-field proximity of the Robbins Island fire (20 km) to Cape Grim, the narrowness of the BB plume and the spatial complexity of the modelled wind fields around north Tasmania are likely to result in strong heterogeneity in the modelled concentrations surrounding Cape

Atmos. Chem. Phys. Discuss., doi:10.5194/acp-2016-932, 2016
Manuscript under review for journal Atmos. Chem. Phys.
Published: 5 December 2016

Grim. We investigated how much model spatial gradients vary by sampling the model output at 4 grid points sited 1 km to the north, east, south and west of Cape Grim. The TAPM-CTM model runs with EF corresponding to the MCE of 0.89 were used for the spatial analysis.

Primary species - CO

Figure 6a shows a time series of the modelled CO output of the difference between Cape Grim and each grid point 1km either side, where plotted CO concentration is other location [CO] (N,S,E,W) –Cape Grim [CO].

The figure clearly shows that there are some large differences in the modelled concentrations of CO between grid points for both BB1 and BB2. Particularly large differences were seen for BB2 with the north gridpoint modelled concentrations in BB2 over 500 ppb lower than at Cape Grim grid point, while at the Southerly grid point the modelled CO was up to 350 ppb higher. Smaller differences of up to 250 ppb between the east and Cape Grim grid points were observed for BB1. This indicates the plume from the fire was narrow and had a highly variably impact on the area immediately surrounding Cape Grim.

Figure 6b shows the observed cumulative concentration of CO over the 56 hour duration of BB2 at Cape Grim, as well as the modelled cumulative concentration at Cape Grim and at the four gridpoints either side. This figure shows both the variability in concentration with location, but also with time. Beyond the 10 hour mark, the model shows major differences in cumulative CO concentrations between the 5 gridpoints (including Cape Grim), highlighting significant spatial variability. For example at the end of BB2 (hour 56), the model predicts that the cumulative modelled CO concentration at Cape Grim is 24% lower than the cumulative concentration 1 km south and 47% higher than the cumulative concentration 1 km north. The modelled cumulative CO concentrations at the South gridpoint at hour 56 is almost twice as high as the north modelled concentration 2 km away (82% difference). This high variability modelled between sites which are closely located highlights the challenges with modelling the impact of a near field fire at a fixed single point location. This also highlights the high spatial variability which may be missed in similar situations by using a coarser resolution model which would dilute emissions in a larger gridbox.

Ozone (O_3)

Figure 6c shows a time series of the modelled O_3 output of the difference between Cape Grim and each gridpoint 1km either side, where plotted O_3 concentration is other location [O_3] (N,S,E,W) – Cape Grim [O_3].

Atmos. Chem. Phys. Discuss., doi:10.5194/acp-2016-932, 2016
Manuscript under review for journal Atmos. Chem. Phys.
Published: 5 December 2016

The modelled concentrations very similar at all grid points when BB emissions are not impacting. The variability increases at the time of BB1 and BB2, with differences mostly within 2-3 ppb, but up to 15 and 10 ppb at east and west sites for BB1. This largest difference corresponds to the additional modelled O_3 peak which showed strong dependency on EF (see Section 3.1.2), and provides further evidence that local BB emissions are driving this enhancement.

The model output for O_3 for BB1 (Figure 7) shows O_3 enhancement downwind of the fire at 11:00 and 13:00 on the 16 February. The very localised and narrow O_3 plume is dispersed by the light (2 m s^{-1}) and variable winds, and Cape Grim is on the edge of the O_3 plume for much of this period, explaining the high variability seen in Figure 6c.

In summary there is a large amount of spatial variability is the model for primary species such as CO during the BB events, with differences of > 500 ppb in grid points 1 km apart. This is due to the close proximity of the fire to the observation site and narrow plume non-stationary meteorology. For O_3, there is up to 15 ppb difference between grid points for a narrow O_3 plume which is formed downwind of the fire.

The highly localised nature of the primary and in some cases secondary species seen here highlights the benefits of assessing spatial variability in situations with a close proximity point source and a fixed receptor (measurement) site. Due to the spatial variability shown for O_3 in BB1, model data from all 5 grid points are reported in Section 3.2.

3.2 Exploring plume chemistry and contribution from different sources

3.2.1 Drivers of O_3 production

In previous work on the Robbins Island fire, it was noted that the increases in O_3 observed after both BB1 and BB2 were correlated with increased concentration of HFC134a. This indicated that transport of photochemically processed air from urban areas to Cape Grim was likely the main driver of the O_3 observed, rather than BB emissions (Lawson et al., 2015). However, an O_3 increase was observed during particle growth (BB1) when urban influence was minimal which suggested O_3 growth may also have been driven by emissions from local fire. Normalised Excess Mixing Ratios (NEMR) observed during BB2 were also in the range of those observed elsewhere in young BB plumes (Lawson et al., 2015).

In this section, we report on how TAPM-CTM was used to determine the degree to which the local fire emissions, and urban emissions, were driving the O_3 enhancements observed.

Atmos. Chem. Phys. Discuss., doi:10.5194/acp-2016-932, 2016
Manuscript under review for journal Atmos. Chem. Phys.
Published: 5 December 2016

Atmospheric Chemistry and Physics Discussions

The model was run using TAPM-CTM with EF corresponding to the lowest MCE of 0.89, as discussioned previously. Three different emission configurations were run to allow identification of BB-driven O_3 formation; a) with all emission sources (E_{all}); b) all emission sources excluding the Robbins Island fire ($E_{exRIfire}$); and c) all emission sources excluding anthropogenic emissions from Melbourne (E_{exMelb}).

The enhancement of O_3 due to emissions from the Robbins Island fire was calculated by

$$E_{RIfire} = E_{all} - E_{exRIfire} \quad (1)$$

The enhancement of O_3 due to emissions from anthropogenic emissions in Melbourne was calculated by

$$E_{Melb} = E_{all} - E_{exMelb} \quad (2)$$

In this way the contribution was estimated from the two most likely sources (emissions from the Robbins Island fire and transported emissions from Melbourne on the Australian mainland).

Due to the high spatial variability of O_3 for BB1 discussed in the previous section, E_{RIfire} and E_{Melb} was calculated for all 5 locations (Cape Grim and 1 km north, south, east and west).

The O_3 modelled times series for the $E_{exRIfire}$ and the E_{exMelb} runs shows distinct O_3 peaks driven by the Robbins Island fire emissions and distict peaks from the Melbourne anthropogenic emissions (Figure 8). The 2 peaks attributed to the fire occur during, or close to the plume strikes, and are short lived (3 and 5 hour) events. These same two peaks showed a strong dependance on model EF in Section 3.1.2. In contrast, the two peaks attributed to transport of air from mainland Australia are of longer duration, and occur after the plume strikes.

The O_3 peaks which were observed following BB1 and BB2 correspond with the modelled O_3 peak in which the Robbins Island fire emissions were switched off, confirming that the origin of the two observed O_3 peaks is transport from mainland Australia, as suggested by the observed HFC-134a. Of the 2 modelled Robbins Island fire-derived O_3 peaks, the first modelled peak (33 ppb) corresponds with a small (21 ppb) observed peak during BB1 (Period B in Lawson et al., 2015), but the second modelled fire-derived O_3 peak is not observed. As shown in Figure 7 and discussed in Section 3.1.3, according to the model the O_3 plumes generated from fire emissions were narrow and showed a strong spatial variability. Given this, it is challenging for the the model to predict the exact timing and magnitude of these highly variable BB generated O_3 peaks impacting Cape Grim. This is likely why there is good agreement in timing and magnitude between model and observations for the large scale,

Atmos. Chem. Phys. Discuss., doi:10.5194/acp-2016-932, 2016
Manuscript under review for journal Atmos. Chem. Phys.
Published: 5 December 2016

Atmospheric Chemistry and Physics Discussions

spatially homogeneous O_3 plumes transported from mainland Australia, but a lesser agreement for the locally formed, spatially variable O_3 formed from local fire emissions.

Given the challenges in modelling narrow locally formed O_3 plumes and the dependence on meteorology in particular, we analysed a longer period surrouding BB1 and BB2 (32 and 71 hours) to remove this temporal variability. We calculated the overall contribution of the Robbins Island fire to total excess (excess to background) O_3 (including anthropogenic O_3) for these periods. To capture some of the spatial variability, model output at the 4 locations around Cape Grim was included in the calculation.

The contribution of the Robbins Island fire emissions to the excess O_3 was calculated by:

$$E_{Rifire} / (E_{Rifire} + E_{Melb}) \times 100 \quad (3)$$

Where the contribution can be positive (O_3 enhanced above background levels) or negative (O_3 depleted below background levels).

Figure 8 shows the modelled contribution of the Robbins Island fire emissions to excess O_3 for the period surrounding BB1 and BB2, where the box and whisker values are the % contributions at each of the 5 sites (Cape Grim and 1 km either side). The model indicates that for an area 4 km^2 surrounding Cape Grim, the Robbins Island fire emissions contributed between 25 to 43% of the total excess O_3 during BB1 and contributed -4 to -6 % to the excess O_3 during BB2. In other words, during BB1, the fire emissions had a net positive contribution to the O_3 in excess of background, while during BB2 the fire emissions had a net destructive effect on the excess O_3. The higher variability in the contribution for BB1 reflects the high spatial variability discussed previously.

In summary, running the model with and without the Robbins Island fire emissions allowed clear separation of the fire-derived O_3 peaks from the anthropogenic derived O_3 peaks, and allowed estimation of the fire contribution to total excess O_3 during BB1 and BB2. While the contributions of BB emissions to O_3 are only estimates due to the issues discussed previously, this work demonstrates how a model can be used to elucidate the degree of contribution from different sources, where this is not possible using observations alone.

3.2.2 Plume age

The model was used to estimate the age of air parcels reaching Cape Grim over the two week period of the Robbins Island fire. The method has been described previously in Keywood et al., (2015). Briefly, two model simulations were run for scenarios which included all sources

Atmos. Chem. Phys. Discuss., doi:10.5194/acp-2016-932, 2016
Manuscript under review for journal Atmos. Chem. Phys.
Published: 5 December 2016

of nitric oxide (NO) in Australia ; the first treated NO as an unreactive tracer, the second with NO decaying at a constant first order rate. The relative fraction of the emitted NO molecules remaining after 96 hours was then inverted to give a molar-weighted plume age.

Figure 9 shows a time series of the modelled NO tracer (decayed version), modelled plume age (hours) and the observed O_3. Direct BB1 and BB2 plume strikes can be clearly seen with increases in NO corresponding with a plume age of 0-2 hours. The plume age then gradually increases over 24 hours in both cases, peaking at 15:00 on the 17th February during BB1 (aged of plume 40 hours) and peaking at 17:00 on the 25th February during BB2 (age of plume 49 hours). The peak observed O_3 enhancements correspond with the simulated plume age in both BB1 and BB2 (with an offset of 2 hours for BB1), and the observed HFC-134a, suggesting that the plume which transported O_3 from Mebourne to Cape Grim was approximately 2 days old. The model also simulates a smaller NO peak alongside the maximum plume age, indicating transport of decayed NO from the mainland to Cape Grim.

As reported in Lawson et al., (2015), during BB2 NEMRs of $\Delta O_3/\Delta CO$ ranged from 0.001-0.074, in agreement with O_3 enhancements observed in young BB plumes elsewhere (Yokelson et al., 2003; Yokelson et al., 2009). However, the modelling reported here suggests that almost all of the O_3 observed during BB2 was of urban, not BB origin. This suggests NEMRs should not be used in isolation to identify the source of observed O_3 enhancements, and highlights the value of utilising air mass back trajectories and modelling to interpret the source of O_3 enhancements where there are multiple emission sources.

3.3 Summary and conclusions

In this work we have used a unique set of opportunistic BB observations at Cape Grim Baseline Air Pollution Station to test the ability of a high resolution (400m grid cell) chemical transport model to reproduce primary (CO, BC) and secondary (O_3) BB species in challenging non-stationary, inhomogeneous, and near field conditions. We tested the sensitivity of the model to three different parameters (meteorology, MCE and spatial variability) while holding the plume rise and the chemical mechanisms constant. We found meteorology, EF and spatial variability have a large influence on the model output mainly due to the close proximity of the fire to the receptor site (Cape Grim). The lower MCE (0.89) TAPM-CTM model simulation provided best agreement with observed concentrations, in agreement with the MCE calculated from observations of 0.88 (Lawson et al., 2015). The changing EFs, in particular NO dependency on MCE, had a major influence on the ability of the model to predict O_3 concentrations, with a

Atmos. Chem. Phys. Discuss., doi:10.5194/acp-2016-932, 2016
Manuscript under review for journal Atmos. Chem. Phys.
Published: 5 December 2016

Atmospheric Chemistry and Physics Discussions

tendency of the model in some configurations to both fail to simulate observed O_3 peaks, and to simulate complete titration of O_3 which was not observed. As shown in the previous work (Lawson et al., 2015), minor rainfall events have the potential to significantly alter EF due to changes in combustion processes. This work suggests that varying model EF has a major impact on whether the model predicts production or destruction of O_3, particularly important at a receptor site in close proximity to the BB emissions. Models which assume a fixed EF for O_3 precursor species in an environment with temporally and spatially variable EF may therefore be challenged to correctly predict the behaviour of important species such as O_3.

There were significant differences in model output between Cape Grim and grid points 1 km away highlighting the narrowness of the plume and the challenge of predicting when the plume would impact the station. This also highlights the high spatial variability which may be missed in similar situations by using a coarser resolution model which would dilute emissions in a larger gridbox.

The model was used to distinguish the influence of the two sources on the observed O_3 enhancements which followed BB1 and BB2. Transport of a 2 day old urban plume some 300km away from Melbourne was the main source of the O_3 enhancement observed at Cape Grim over the two week period of the fire. The model suggests the Robbins Island fire contributed approximately 25-43% of observed O_3 to the BB1 O_3 enhancement, but for BB2 the fire caused a net O_3 depletion below background levels. Despite NEMRs of $\Delta O_3/\Delta CO$ during BB2 being similar to that observed in young BB plumes elsewhere, this work suggests NEMRs should not be used in isolation to identify the source of observed O_3 enhancements, and highlights the value of utilising air mass back trajectories and modelling to interpret the source of O_3 enhancements where there are multiple emission sources.

Acknowledgements

The Cape Grim program, established by the Australian Government to monitor and study global atmospheric composition, is a joint responsibility of the Bureau of Meteorology (BOM) and the Commonwealth Scientific and Industrial Research Organisation (CSIRO). We thank the staff at Cape Grim and staff at CSIRO Oceans and Atmosphere for providing observation data for this work. Thank you to Nada Derek for producing figures.

Atmos. Chem. Phys. Discuss., doi:10.5194/acp-2016-932, 2016
Manuscript under review for journal Atmos. Chem. Phys.
Published: 5 December 2016

Atmospheric Chemistry and Physics Discussions

References

Akagi, S. K., Yokelson, R. J., Burling, I. R., Meinardi, S., Simpson, I., Blake, D. R., McMeeking, G. R., Sullivan, A., Lee, T., Kreidenweis, S., Urbanski, S., Reardon, J., Griffith, D. W. T., Johnson, T. J., and Weise, D. R.: Measurements of reactive trace gases and variable O3 formation rates in some South Carolina biomass burning plumes, Atmos. Chem. Phys., 13, 1141-1165, 10.5194/acp-13-1141-2013, 2013.

Alvarado, M. J., and Prinn, R. G.: Formation of ozone and growth of aerosols in young smoke plumes from biomass burning: 1. Lagrangian parcel studies, Journal of Geophysical Research, 114, 10.1029/2008jd011144, 2009.

Alvarado, M. J., Wang, C., and Prinn, R. G.: Formation of ozone and growth of aerosols in young smoke plumes from biomass burning: 2. Three-dimensional Eulerian studies, Journal of Geophysical Research, 114, 10.1029/2008jd011186, 2009.

Alvarado, M. J., Lonsdale, C. R., Yokelson, R. J., Akagi, S. K., Coe, H., Craven, J. S., Fischer, E. V., McMeeking, G. R., Seinfeld, J. H., Soni, T., Taylor, J. W., Weise, D. R., and Wold, C. E.: Investigating the links between ozone and organic aerosol chemistry in a biomass burning plume from a prescribed fire in California chaparral, Atmos. Chem. Phys., 15, 6667-6688, 10.5194/acp-15-6667-2015, 2015.

Anderson, D. C., Nicely, J. M., Salawitch, R. J., Canty, T. P., Dickerson, R. R., Hanisco, T. F., Wolfe, G. M., Apel, E. C., Atlas, E., Bannan, T., Bauguitte, S., Blake, N. J., Bresch, J. F., Campos, T. L., Carpenter, L. J., Cohen, M. D., Evans, M., Fernandez, R. P., Kahn, B. H., Kinnison, D. E., Hall, S. R., Harris, N. R., Hornbrook, R. S., Lamarque, J. F., Le Breton, M., Lee, J. D., Percival, C., Pfister, L., Pierce, R. B., Riemer, D. D., Saiz-Lopez, A., Stunder, B. J., Thompson, A. M., Ullmann, K., Vaughan, A., and Weinheimer, A. J.: A pervasive role for biomass burning in tropical high ozone/low water structures, Nature communications, 7, 10267, 10.1038/ncomms10267, 2016.

Andreae, M. O., and Merlet, P.: Emission of trace gases and aerosols from biomass burning, Global Biogeochemical Cycles, 15, 955-966, 10.1029/2000gb001382, 2001.

Andreae, M. O., Artaxo, P., Brandao, C., Carswell, F. E., Ciccioli, P., da Costa, A. L., Culf, A. D., Esteves, J. L., Gash, J. H. C., Grace, J., Kabat, P., Lelieveld, J., Malhi, Y., Manzi, A. O., Meixner, F. X., Nobre, A. D., Nobre, C., Ruivo, M., Silva-Dias, M. A., Stefani, P., Valentini, R., von Jouanne, J., and Waterloo, M. J.: Biogeochemical cycling of carbon, water, energy, trace gases, and aerosols in Amazonia: The LBA-EUSTACH experiments, Journal of Geophysical Research-Atmospheres, 107, 8066 10.1029/2001jd000524, 2002.

Arnold, S. R., Emmons, L. K., Monks, S. A., Law, K. S., Ridley, D. A., Turquety, S., Tilmes, S., Thomas, J. L., Bouarar, I., Flemming, J., Huijnen, V., Mao, J., Duncan, B. N., Steenrod, S., Yoshida, Y., Langner, J., and Long, Y.: Biomass burning influence on high-latitude tropospheric ozone and reactive nitrogen in summer 2008: a multi-model analysis based on POLMIP simulations, Atmospheric Chemistry and Physics, 15, 6047-6068, 10.5194/acp-15-6047-2015, 2015.

Artaxo, P., Rizzo, L. V., Brito, J. F., Barbosa, H. M. J., Arana, A., Sena, E. T., Cirino, G. G., Bastos, W., Martin, S. T., and Andreae, M. O.: Atmospheric aerosols in Amazonia and land use change: from natural biogenic to biomass burning conditions, Faraday Discuss., 165, 203-235, 10.1039/c3fd00052d, 2013.

Azzi, M., Cope, M., and Rae, M.: Sustainable Energy Deployment within the Greater Metropolitan Region. NSW- Environmental Trust 2012.

Barrett, D. J.: Steady state turnover time of carbon in the Australian terrestrial biosphere, Global Biogeochemical Cycles, 16, 55-51-55-21, 10.1029/2002gb001860, 2002.

Broome, R. A., Cope, M. E., Goldsworthy, B., Goldsworthy, L., Emmerson, K., Jegasothy, E., and Morgan, G. G.: The mortality effect of ship-related fine particulate matter in the Sydney greater metropolitan region of NSW, Australia, Environment International, 87, 85-93, http://dx.doi.org/10.1016/j.envint.2015.11.012, 2016.

Cope, M., Lee, S., Noonan, J., Lilley, B., Hess, G. D., and Azzi, M.: Chemical Transport Model - Technical Description, 2009.

Cope, M., Keywood, M., Emmerson, K., Galbally, I. E., Boast, K., Chambers, S., Cheng, M., Crumeyrolle, S., Dunne, E., Fedele, R., Gillett, R., Griffiths, A., Harnwell, J., Katzfey, J., Hess, D., Lawson, S. J., Miljevic, B., Molloy, S., Powell, J., Reisen, F., Ristovski, Z., Selleck, P., Ward, J., Zhang, C., and Zeng, J.: Sydney Particle Study Stage II., 2014. http://141.243.32.146/resources/aqms/SydParticleStudy10-13.pdf

Cope, M. E., Hess, G. D., Lee, S., Tory, K., Azzi, M., Carras, J., Lilley, W., Manins, P. C., Nelson, P., Ng, L., Puri, K., Wong, N., Walsh, S., and Young, M.: The Australian Air Quality Forecasting System. Part I: Project Description and Early Outcomes, Journal of Applied Meteorology, 43, 649-662, doi:10.1175/2093.1, 2004.

Delaney, W., and Marshall, A. G.: Victorian Air Emissions Inventory for 2006, 20th International Clean Air and Environment Conference, Auckland,, 2011.

Dennekamp, M., Straney, L. D., Erbas, B., Abramson, M. J., Keywood, M., Smith, K., Sim, M. R., Glass, D. C., Del Monaco, A., Haikerwal, A., and Tonkin, A. M.: Forest Fire Smoke Exposures and Out-of-Hospital Cardiac Arrests in Melbourne, Australia: A Case-Crossover Study, Environmental health perspectives, 123, 959-964, 10.1289/ehp.1408436, 2015.

Donahue, N. M., Robinson, A. L., Stanier, C. O., and Pandis, S. N.: Coupled Partitioning, Dilution, and Chemical Aging of Semivolatile Organics, Environmental Science & Technology, 40, 2635-2643, 10.1021/es052297c, 2006.

Draxler, R.R and Hess, G.D. .: Description of the HYSPLIT_4 modeling system. NOAA Technical Memorandum ERL ARL-224, Air Resources Laboratory Silver Spring, Maryland, USA, 1997.

Emmerson, K. M., Galbally, I. E., Guenther, A. B., Paton-Walsh, C., Guerette, E. A., Cope, M. E., Keywood, M. D., Lawson, S. J., Molloy, S. B., Dunne, E., Thatcher, M., Karl, T., and Maleknia, S. D.: Current estimates of biogenic emissions from eucalypts uncertain for southeast Australia, Atmos. Chem. Phys., 16, 6997-7011, 10.5194/acp-16-6997-2016, 2016.

Emmons, L. K., Apel, E. C., Lamarque, J. F., Hess, P. G., Avery, M., Blake, D., Brune, W., Campos, T., Crawford, J., DeCarlo, P. F., Hall, S., Heikes, B., Holloway, J., Jimenez, J. L., Knapp, D. J., Kok, G., Mena-Carrasco, M., Olson, J., O'Sullivan, D., Sachse, G., Walega, J., Weibring, P., Weinheimer, A., and Wiedinmyer, C.: Impact of Mexico City emissions on regional air quality from MOZART-4 simulations, Atmospheric Chemistry and Physics, 10, 6195-6212, 10.5194/acp-10-6195-2010, 2010.

Ferek, R. J., Reid, J. S., Hobbs, P. V., Blake, D. R., and Liousse, C.: Emission factors of hydrocarbons, halocarbons, trace gases and particles from biomass burning in Brazil, Journal of Geophysical Research: Atmospheres, 103, 32107-32118, 10.1029/98JD00692, 1998.

Flannigan, M. D., Krawchuk, M. A., de Groot, W. J., Wotton, B. M., and Gowman, L. M.: Implications of changing climate for global wildland fire, International Journal of Wildland Fire, 18, 483-507, http://dx.doi.org/10.1071/WF08187, 2009.

Fountoukis, C., and Nenes, A.: ISORROPIA II: a computationally efficient thermodynamic equilibrium model for K+-Ca2+-Mg2+-Nh(4)(+)-Na+-SO42--NO3--Cl--H2O aerosols, Atmos Chem Phys, 7, 4639-4659, 2007.

Freitas, S. R., Longo, K. M., Chatfield, R., Latham, D., Silva Dias, M. A. F., Andreae, M. O., Prins, E., Santos, J. C., Gielow, R., and Carvalho Jr, J. A.: Including the sub-grid scale plume rise of vegetation fires in low resolution atmospheric transport models, Atmos. Chem. Phys., 7, 3385-3398, 10.5194/acp-7-3385-2007, 2007.

Galbally, I. E., Cope, M., Lawson, S. J., Bentley, S. T., Cheng, M., Gillet, R. W., Selleck, P., Petraitis, B., Dunne, E., and Lee, S.: Sources of Ozone Precursors and Atmospheric Chemistry in a Typical Australian City, 2008. http://olr.npi.gov.au/atmosphere/airquality/publications/pubs/ozone-precursors.pdf

Gong, S. L.: A parameterization of sea-salt aerosol source function for sub- and super-micron particles, Global Biogeochem Cy, 17, Artn 1097 Doi 10.1029/2003gb002079, 2003.

Goodrick, S. L., Achtemeier, G. L., Larkin, N. K., Liu, Y., and Strand, T. M.: Modelling smoke transport from wildland fires: a review, International Journal of Wildland Fire, 22, 83, 10.1071/wf11116, 2013.

Hecobian, A., Liu, Z., Hennigan, C. J., Huey, L. G., Jimenez, J. L., Cubison, M. J., Vay, S., Diskin, G. S., Sachse, G. W., Wisthaler, A., Mikoviny, T., Weinheimer, A. J., Liao, J., Knapp, D. J., Wennberg, P. O., Kurten, A., Crounse, J. D., St Clair, J., Wang, Y., and Weber, R. J.: Comparison of chemical characteristics of 495 biomass burning plumes intercepted by the NASA DC-8 aircraft during the ARCTAS/CARB-2008 field campaign, Atmospheric Chemistry and Physics, 11, 13325-13337, 10.5194/acp-11-13325-2011, 2012.

Hess, G. D.: A photochemical model for air quality assessment: Model description and verification, Atmospheric Environment (1967), 23, 643-660, http://dx.doi.org/10.1016/0004-6981(89)90013-9, 1989.

Hurley, P.: Development and Verification of TAPM, in: Air Pollution Modeling and Its Application XIX, edited by: Borrego, C., and Miranda, A. I., Springer Netherlands, Dordrecht, 208-216, 2008a.

Hurley, P. J.: TAPM V4. Part 1. Technical description, CSIRO Marine and Atmospheric Research Internal Report, 2008b.

Jaffe, D. A., and Wigder, N. L.: Ozone production from wildfires: A critical review, Atmospheric Environment, 51, 1-10, 10.1016/j.atmosenv.2011.11.063, 2012.

Jost, C., Trentmann, J., Sprung, D., Andreae, M. O., McQuaid, J. B., and Barjat, H.: Trace gas chemistry in a young biomass burning plume over Namibia: Observations and model simulations, Journal of Geophysical Research-Atmospheres, 108, 13, 8482 10.1029/2002jd002431, 2003.

Kaiser, J. W., Heil, A., Andreae, M. O., Benedetti, A., Chubarova, N., Jones, L., Morcrette, J. J., Razinger, M., Schultz, M. G., Suttie, M., and van der Werf, G. R.: Biomass burning emissions estimated with a global fire assimilation system based on observed fire radiative power, Biogeosciences, 9, 527-554, 10.5194/bg-9-527-2012, 2012.

Keywood, M., Guyes, H., Selleck, P., and Gillett, R.: Quantification of secondary organic aerosol in an Australian urban location, Environmental Chemistry, 8, 115-126, 10.1071/en10100, 2011a.

Keywood, M., Kanakidou, M., Stohl, A., Dentener, F., Grassi, G., Meyer, C. P., Torseth, K., Edwards, D., Thompson, A., Lohmann, U., and Burrows, J. P.: Fire in the Air- Biomass burning impacts in a changing climate, Critical Reviews in Environmental Science and Technology, DOI:10.1080/10643389.2011.6042482011b.

Keywood, M., Cope, M., Meyer, C. P. M., Iinuma, Y., and Emmerson, K.: When smoke comes to town: The impact of biomass burning smoke on air quality, Atmospheric Environment, 121, 13-21, http://dx.doi.org/10.1016/j.atmosenv.2015.03.050, 2015.

Lawson, S. J., Keywood, M. D., Galbally, I. E., Gras, J. L., Cainey, J. M., Cope, M. E., Krummel, P. B., Fraser, P. J., Steele, L. P., Bentley, S. T., Meyer, C. P., Ristovski, Z., and Goldstein, A. H.: Biomass burning emissions of trace gases and particles in marine air at Cape Grim, Tasmania, Atmos. Chem. Phys., 15, 13393-13411, 10.5194/acp-15-13393-2015, 2015.

Lei, W., Li, G., and Molina, L. T.: Modeling the impacts of biomass burning on air quality in and around Mexico City, Atmospheric Chemistry and Physics, 13, 2299-2319, 10.5194/acp-13-2299-2013, 2013.

Lu, H., and Shao, Y. P.: A new model for dust emission by saltation bombardment, J Geophys Res-Atmos, 104, 16827-16841, Doi 10.1029/1999jd900169, 1999.

Luhar, A. K., Mitchell, R. M., Meyer, C. P., Qin, Y., Campbell, S., Gras, J. L., and Parry, D.: Biomass burning emissions over northern Australia constrained by aerosol measurements: II—Model validation, and impacts on air quality and radiative forcing, Atmospheric Environment, 42, 1647-1664, http://dx.doi.org/10.1016/j.atmosenv.2007.12.040, 2008.

Mason, S. A., Trentmann, J., Winterrath, T., Yokelson, R. J., Christian, T. J., Carlson, L. J., Warner, T. R., Wolfe, L. C., and Andreae, M. O.: Intercomparison of Two Box Models of the Chemical Evolution in Biomass-Burning Smoke Plumes, Journal of Atmospheric Chemistry, 55, 273-297, 10.1007/s10874-006-9039-5, 2006.

McGregor, J. L.: Recent developments in variable-resolution global climate modelling, Climatic Change, 129, 369-380, 10.1007/s10584-013-0866-5, 2015.

Meyer, C. P., Luhar, A. K., and Mitchell, R. M.: Biomass burning emissions over northern Australia constrained by aerosol measurements: I—Modelling the distribution of hourly emissions, Atmospheric Environment, 42, 1629-1646, http://dx.doi.org/10.1016/j.atmosenv.2007.10.089, 2008.

Ortega, A. M., Day, D. A., Cubison, M. J., Brune, W. H., Bon, D., de Gouw, J. A., and Jimenez, J. L.: Secondary organic aerosol formation and primary organic aerosol oxidation from biomass-burning smoke in a flow reactor during FLAME-3, Atmospheric Chemistry and Physics, 13, 11551-11571, 10.5194/acp-13-11551-2013, 2013.

Pacifico, F., Folberth, G. A., Sitch, S., Haywood, J. M., Rizzo, L. V., Malavelle, F. F., and Artaxo, P.: Biomass burning related ozone damage on vegetation over the Amazon forest: a model sensitivity study, Atmos. Chem. Phys., 15, 2791-2804, 10.5194/acp-15-2791-2015, 2015.

Parrington, M., Palmer, P. I., Henze, D. K., Tarasick, D. W., Hyer, E. J., Owen, R. C., Helmig, D., Clerbaux, C., Bowman, K. W., Deeter, M. N., Barratt, E. M., Coheur, P. F., Hurtmans, D., Jiang, Z., George, M., and Worden, J. R.: The influence of boreal biomass burning emissions on the distribution of tropospheric ozone over North America and the North Atlantic during 2010, Atmospheric Chemistry and Physics, 12, 2077-2098, 10.5194/acp-12-2077-2012, 2012.

Paugam, R., Wooster, M., Freitas, S., and Val Martin, M.: A review of approaches to estimate wildfire plume injection height within large-scale atmospheric chemical transport models, Atmos. Chem. Phys., 16, 907-925, 10.5194/acp-16-907-2016, 2016.

Reid, C. E., Brauer, M., Johnston, F. H., Jerrett, M., Balmes, J. R., and Elliott, C. T.: Critical Review of Health Impacts of Wildfire Smoke Exposure, Environmental health perspectives, 124, 1334-1343, 10.1289/ehp.1409277, 2016.

Reid, J. S., Hyer, E. J., Prins, E. M., Westphal, D. L., Zhang, J., Wang, J., Christopher, S. A., Curtis, C. A., Schmidt, C. C., Eleuterio, D. P., Richardson, K. A., and Hoffman, J. P.: Global Monitoring and Forecasting of Biomass-Burning Smoke: Description of and Lessons From the Fire Locating and Modeling of Burning Emissions (FLAMBE) Program, IEEE Journal of Selected Topics in Applied Earth Observations and Remote Sensing, 2, 144-162, 10.1109/JSTARS.2009.2027443, 2009.

Reisen, F., Meyer, C. P., McCaw, L., Powell, J. C., Tolhurst, K., Keywood, M. D., and Gras, J. L.: Impact of smoke from biomass burning on air quality in rural communities in southern Australia, Atmospheric Environment, 45, 3944-3953, 10.1016/j.atmosenv.2011.04.060, 2011.

Reisen, F., Duran, S. M., Flannigan, M., Elliott, C., and Rideout, K.: Wildfire smoke and public health risk, International Journal of Wildland Fire, 24, 1029, 10.1071/wf15034, 2015.

Sarwar, G., Luecken, D., Yarwood, G., Whitten, G. Z., and Carter, W. P. L.: Impact of an updated carbon bond mechanism on predictions from the CMAQ modeling system: Preliminary assessment, J Appl Meteorol Clim, 47, 3-14, Doi 10.1175/2007jamc1393.1, 2008.

Sarwar, G., Appel, K. W., Carlton, A. G., Mathur, R., Schere, K., Zhang, R., and Majeed, M. A.: Impact of a new condensed toluene mechanism on air quality model predictions in the US, Geosci Model Dev, 4, 183-193, DOI 10.5194/gmd-4-183-2011, 2011.

Seinfeld, J. H., and Pandis, S. N.: Atmospheric chemistry and physics : from air pollution to climate change, Wiley, New York, xxvii, 1326 p. pp., 1998.

Smagorinsky, J.: General circulation experiments with the primitive equations Monthly Weather Review, 91, 99-164, doi:10.1175/1520-0493(1963)091<0099:GCEWTP>2.3.CO;2, 1963.

Trentmann, J., Yokelson, R. J., Hobbs, P. V., Winterrath, T., Christian, T. J., Andreae, M. O., and Mason, S. A.: An analysis of the chemical processes in the smoke plume from a savanna fire, Journal of Geophysical Research-Atmospheres, 110, 20, D12301 10.1029/2004jd005628, 2005.

Tsimpidi, A. P., Karydis, V. A., Zavala, M., Lei, W., Molina, L., Ulbrich, I. M., Jimenez, J. L., and Pandis, S. N.: Evaluation of the volatility basis-set approach for the simulation of organic aerosol formation in the Mexico City metropolitan area, Atmos Chem Phys, 10, 525-546, 2010.

van Leeuwen, T. T., and van der Werf, G. R.: Spatial and temporal variability in the ratio of trace gases emitted from biomass burning, Atmospheric Chemistry and Physics, 11, 3611-3629, 10.5194/acp-11-3611-2011, 2011.

Walcek, C. J.: Minor flux adjustment near mixing ratio extremes for simplified yet highly accurate monotonic calculation of tracer advection, Journal of Geophysical Research: Atmospheres, 105, 9335-9348, 10.1029/1999JD901142, 2000.

Wigder, N. L., Jaffe, D. A., and Saketa, F. A.: Ozone and particulate matter enhancements from regional wildfires observed at Mount Bachelor during 2004-2011, Atmospheric Environment, 75, 24-31, 10.1016/j.atmosenv.2013.04.026, 2013.

Yokelson, R. J., Bertschi, I. T., Christian, T. J., Hobbs, P. V., Ward, D. E., and Hao, W. M.: Trace gas measurements in nascent, aged, and cloud-processed smoke from African savanna fires by airborne Fourier transform infrared spectroscopy (AFTIR), Journal of Geophysical Research-Atmospheres, 108, 8478 10.1029/2002jd002322, 2003.

Yokelson, R. J., Karl, T., Artaxo, P., Blake, D. R., Christian, T. J., Griffith, D. W. T., Guenther, A., and Hao, W. M.: The Tropical Forest and Fire Emissions Experiment: overview and airborne fire emission factor measurements, Atmospheric Chemistry and Physics, 7, 5175-5196, 2007.

Yokelson, R. J., Crounse, J. D., DeCarlo, P. F., Karl, T., Urbanski, S., Atlas, E., Campos, T., Shinozuka, Y., Kapustin, V., Clarke, A. D., Weinheimer, A., Knapp, D. J., Montzka, D. D., Holloway, J., Weibring, P., Flocke, F., Zheng, W., Toohey, D., Wennberg, P. O., Wiedinmyer, C., Mauldin, L., Fried, A., Richter, D., Walega, J., Jimenez, J. L., Adachi, K., Buseck, P. R., Hall, S. R., and Shetter, R.: Emissions from biomass burning in the Yucatan, Atmospheric Chemistry and Physics, 9, 5785-5812, 2009.

Yokelson, R. J., Burling, I. R., Urbanski, S. P., Atlas, E. L., Adachi, K., Buseck, P. R., Wiedinmyer, C., Akagi, S. K., Toohey, D. W., and Wold, C. E.: Trace gas and particle emissions from open biomass burning in Mexico, Atmospheric Chemistry and Physics, 11, 6787-6808, 10.5194/acp-11-6787-2011, 2011.

Atmos. Chem. Phys. Discuss., doi:10.5194/acp-2016-932, 2016
Manuscript under review for journal Atmos. Chem. Phys.
Published: 5 December 2016

Atmospheric Chemistry and Physics Discussions

Table 1. EF used in sensitivity studies, corresponding to low, medium and high MCEs. A subset of the total species included in the CB05 lumped chemical mechanism are shown. NO = nitric oxide, CO =carbon monoxide, PAR=paraffin carbon bond, OLE= terminal olefin carbon bond, TOL=toluene and other monoalkyl aromatics, XYL=xylene and other polyalkyl aromatics, BNZ =benzene, FORM=formaldehyde, ALD2=acetaldehyde, EC25=elemental carbon <2.5 µm, OC=primary organic carbon < 2.5 µm

	EF g kg $^{-1}$		
	MCE 0.89	MCE 0.92	MCE 0.95
NO	0.8	2.7	4.7
CO	121	89	57
PAR	2.33	2.02	1.40
OLE	0.81	0.7	0.49
TOL	0.3	0.26	0.18
XYL	0.07	0.06	0.04
BNZ	0.35	0.3	0.21
FORM	0.63	0.55	0.38
ALD2	0.75	0.65	0.45
EC25	0.16	0.29	0.45
OC25	4.34	3.47	2.60

Atmos. Chem. Phys. Discuss., doi:10.5194/acp-2016-932, 2016
Manuscript under review for journal Atmos. Chem. Phys.
Published: 5 December 2016

Atmospheric Chemistry and Physics Discussions

Table 2. Summary of sensitivity study results, including Meteorology, Emission Factors and Spatial Variability.

Sensitivity study	Species	TAPM-CTM simulation	CCAM-CTM simulation	Comments/drivers of model outputs
Meteorology (Section 3.1.1)	BC and CO	BB1 plume strike +3 hr Duration 12 hr (actual 5 hr)	BB1 plume strike -12 hr Duration 36 hr intermittent (actual 5 hr)	Narrow BB plume. Differences in plume strike due to timing and duration driven by timing of wind direction change, windspeeds
		BB2 plume strike 0 hr Duration 50 hr (actual 57 hr)	BB2 plume strike 0 hr Duration 57 hr (actual 57 hr)	Concentrations driven by directness of plume hit and PBL height
	O_3	4 O_3 peaks simulated (2 observed, 2 not)	1 O_3 peak simulated (observed)	Dilution of precursors due to dispersion and PBL height (and EF – see below)
Emission Factors (Section 3.1.2)	BC and CO	BC peak magnitude varies by factor 3, CO factor 2 with different EF runs	As for TAPM -CTM	Concentrations vary according to EF input ratios.
	O_3	2 peaks with high EF sensitivity, 2 peaks with no EF sensitivity	1 peak with no EF sensitivity	NO EF (varies with MCE) drives destruction or production of O_3 in fire related peaks. MCE 0.89 TAPM-CTM simulation gives best agreement with observations
Spatial Variability (Section 3.1.3)	CO	Differences of up to > 500 ppb in grid points 1 km apart (BB2)	n/a	Narrow BB plume
	O_3	Differences of up to 15 ppb in grid points 1 km apart (BB1)	n/a	Narrow ozone plume generated downwind of fire

Atmos. Chem. Phys. Discuss., doi:10.5194/acp-2016-932, 2016
Manuscript under review for journal Atmos. Chem. Phys.
Published: 5 December 2016

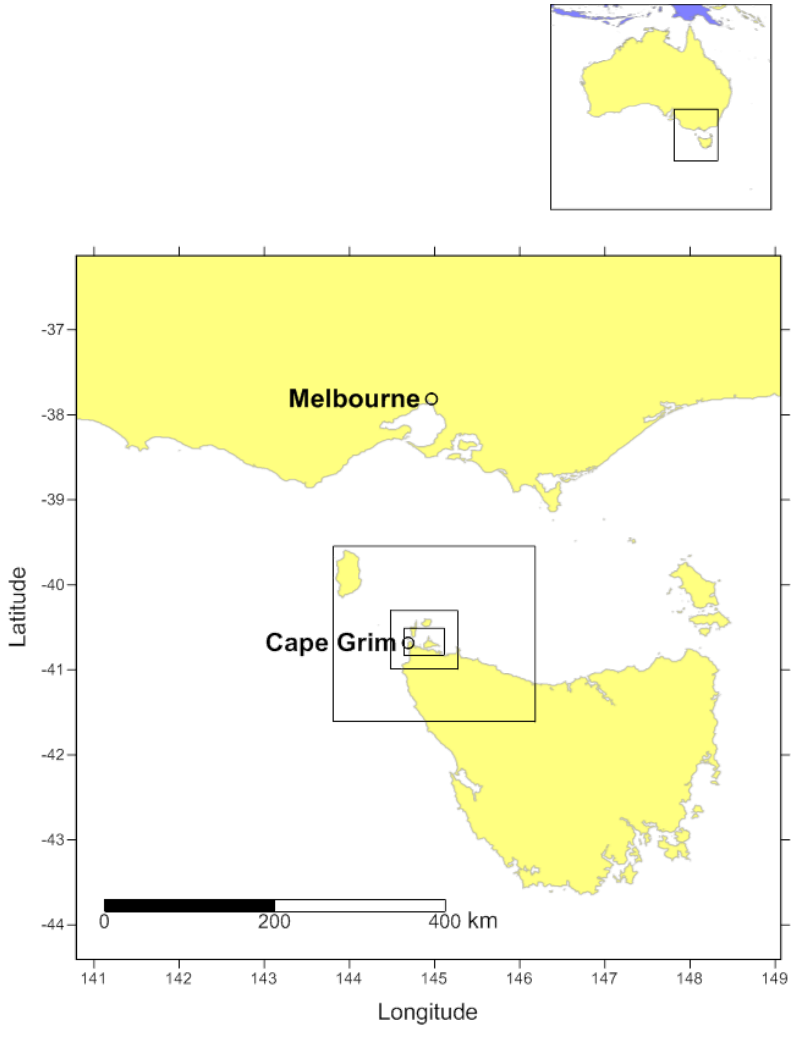

Figure 1. The five nested computational domains used in the model, showing cell spacings of 20 km, 12 km, 3 km, 1 km and 400 m.

Atmos. Chem. Phys. Discuss., doi:10.5194/acp-2016-932, 2016
Manuscript under review for journal Atmos. Chem. Phys.
Published: 5 December 2016

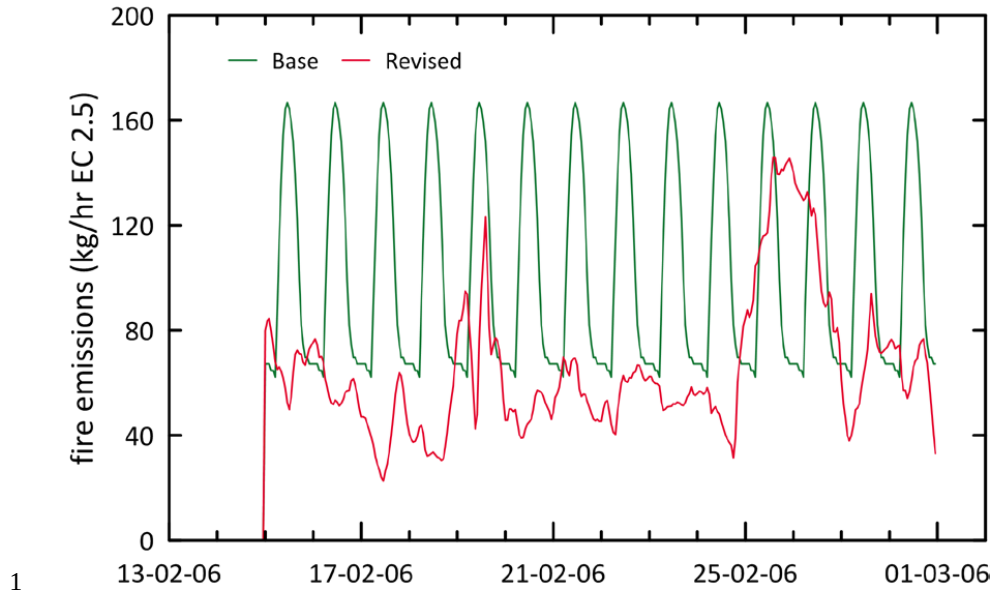

Figure 2. Base hourly diurnal emissions and revised emissions calculated using the Macarthur Fire Danger Index (FDI), in which the presence of strong winds results in faster fire spread and enhanced emissions. Revised emissions were used in all simulations.

Atmos. Chem. Phys. Discuss., doi:10.5194/acp-2016-932, 2016
Manuscript under review for journal Atmos. Chem. Phys.
Published: 5 December 2016

Atmospheric Chemistry and Physics Discussions

1

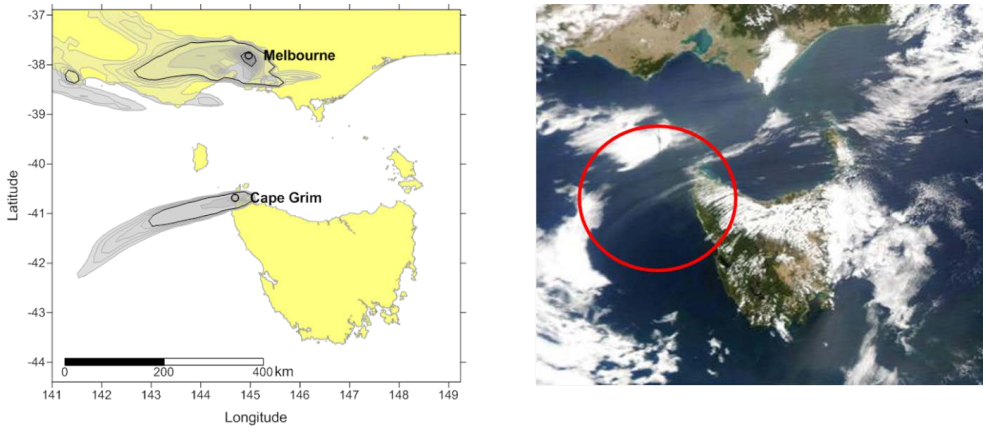

2

3 **Figure 3. Model output of BC (left) on the 23rd February, with a MODIS Truecolour image of the same**
4 **period.**

Atmos. Chem. Phys. Discuss., doi:10.5194/acp-2016-932, 2016
Manuscript under review for journal Atmos. Chem. Phys.
Published: 5 December 2016

Atmospheric Chemistry and Physics Discussions

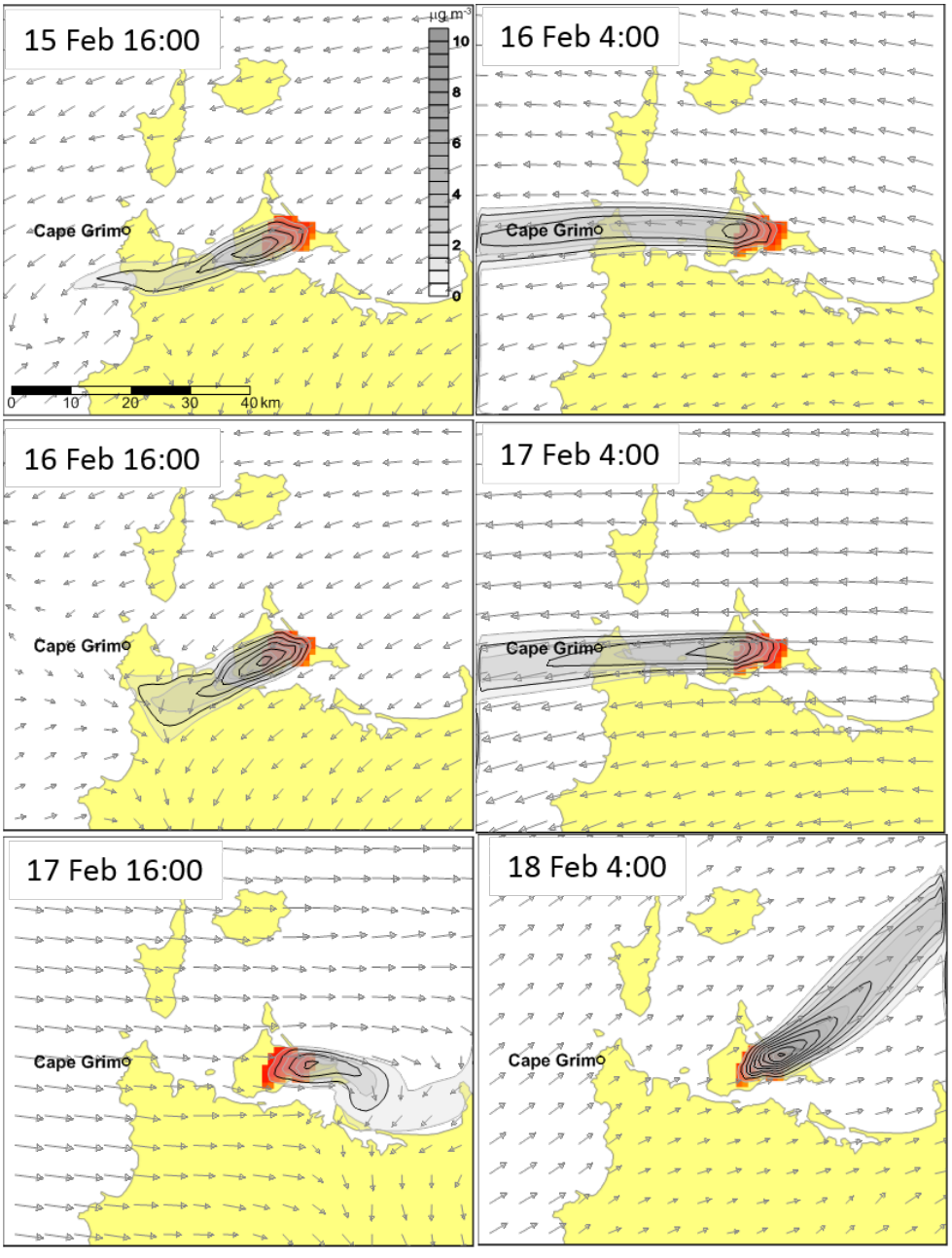

Figure 4. Model output of BC for CCAM-CTM at 12 hour time intervals during BB1, showing the Robbins Island BB plume strike intermittently striking Cape Grim (until 17 Feb 4:00), and then the change in plume direction with wind direction change.

Atmos. Chem. Phys. Discuss., doi:10.5194/acp-2016-932, 2016
Manuscript under review for journal Atmos. Chem. Phys.
Published: 5 December 2016

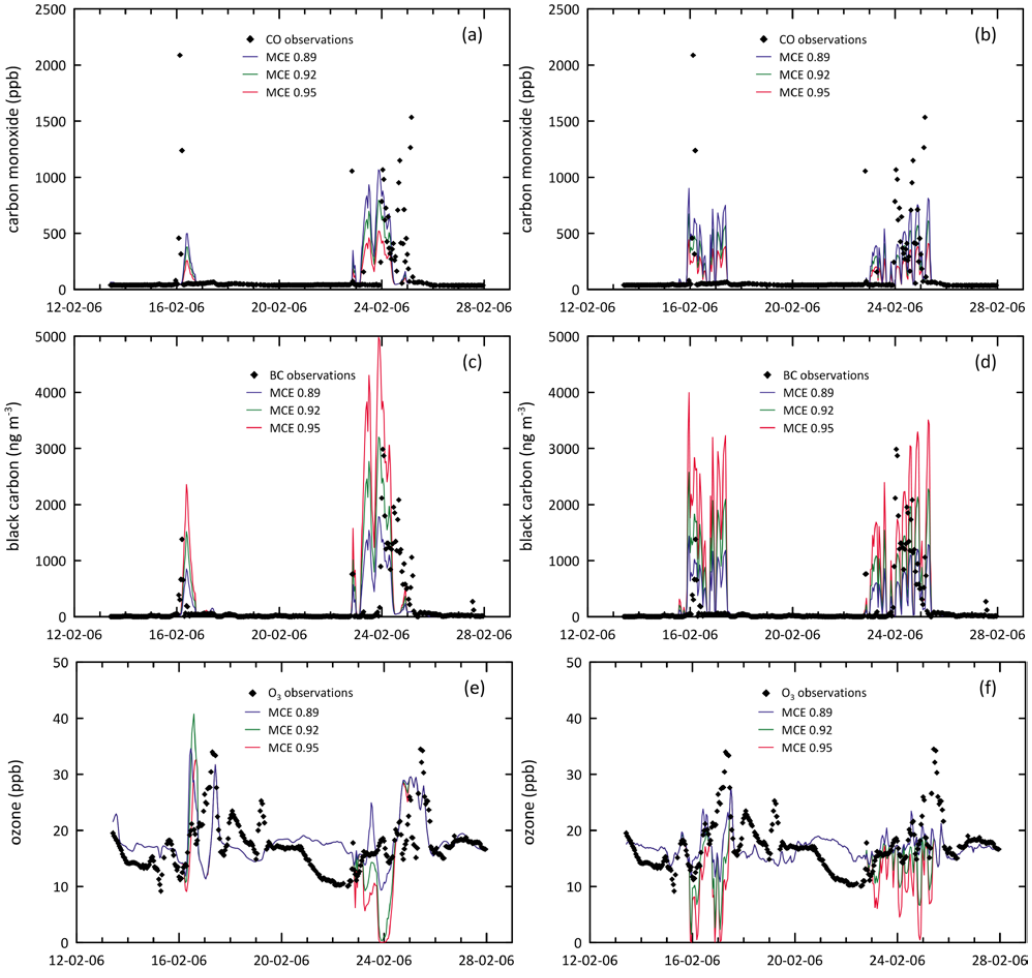

Figure 5. Simulated CO using a) TAPM-CTM and b) CCAM-CTM; simulated BC using c) TAPM-CTM and d) CCAM-CTM and simulated O_3 using e) TAPM-CTM and f) CCAM-CTM. Coloured lines represent different MCE EF simulations, black symbols are observations

Atmos. Chem. Phys. Discuss., doi:10.5194/acp-2016-932, 2016
Manuscript under review for journal Atmos. Chem. Phys.
Published: 5 December 2016

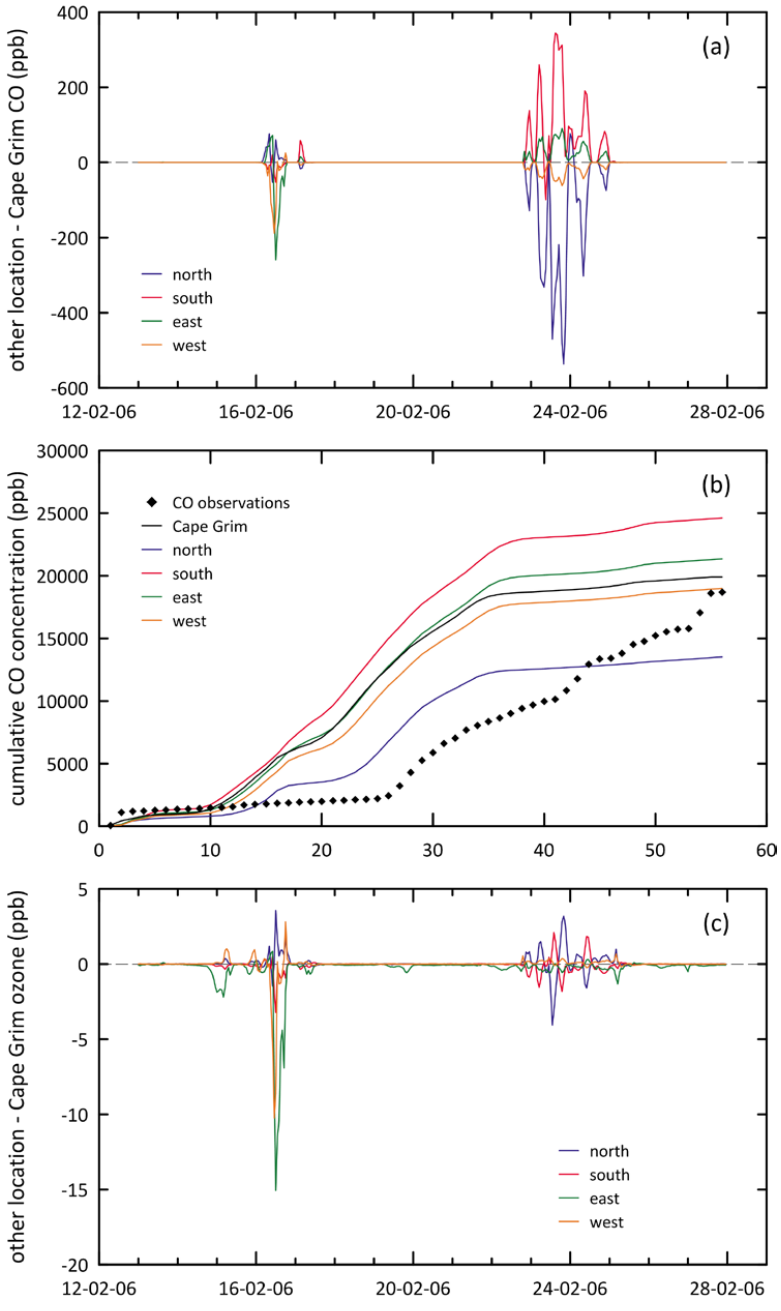

Figure 6. Simulated spatial variability showing a) time series of CO b) cumulative CO and c) time series of O_3. All plots show 4 grid points surrounding Cape Grim over two weeks of fire (BB1 and BB2 shown). Observations are black symbols.

Atmos. Chem. Phys. Discuss., doi:10.5194/acp-2016-932, 2016
Manuscript under review for journal Atmos. Chem. Phys.
Published: 5 December 2016

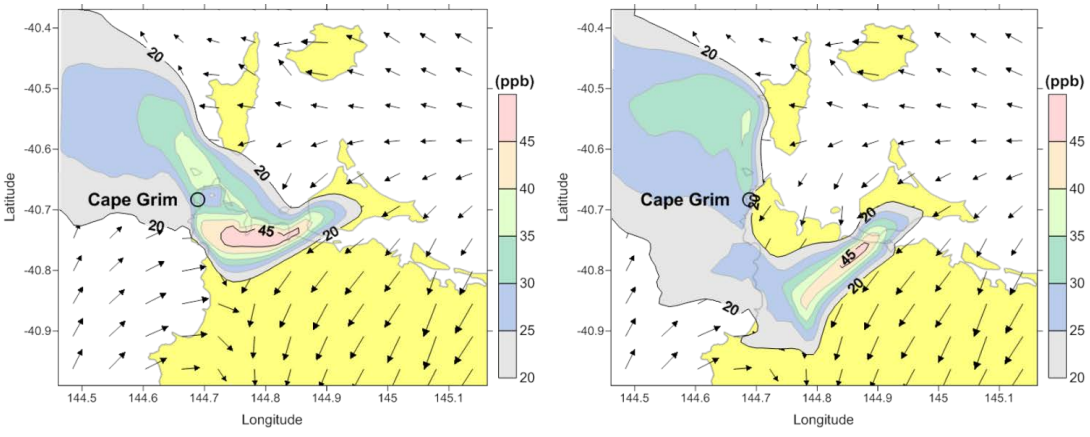

Figure 7. O_3 enhancement downwind of the fire during BB1 at 11:00 and 13:00 on the 16 February, for TAPM-CTM including fire and Melbourne emissions. The spatially variable plume and complex wind fields are shown.

Atmos. Chem. Phys. Discuss., doi:10.5194/acp-2016-932, 2016
Manuscript under review for journal Atmos. Chem. Phys.
Published: 5 December 2016

Atmospheric Chemistry and Physics Discussions

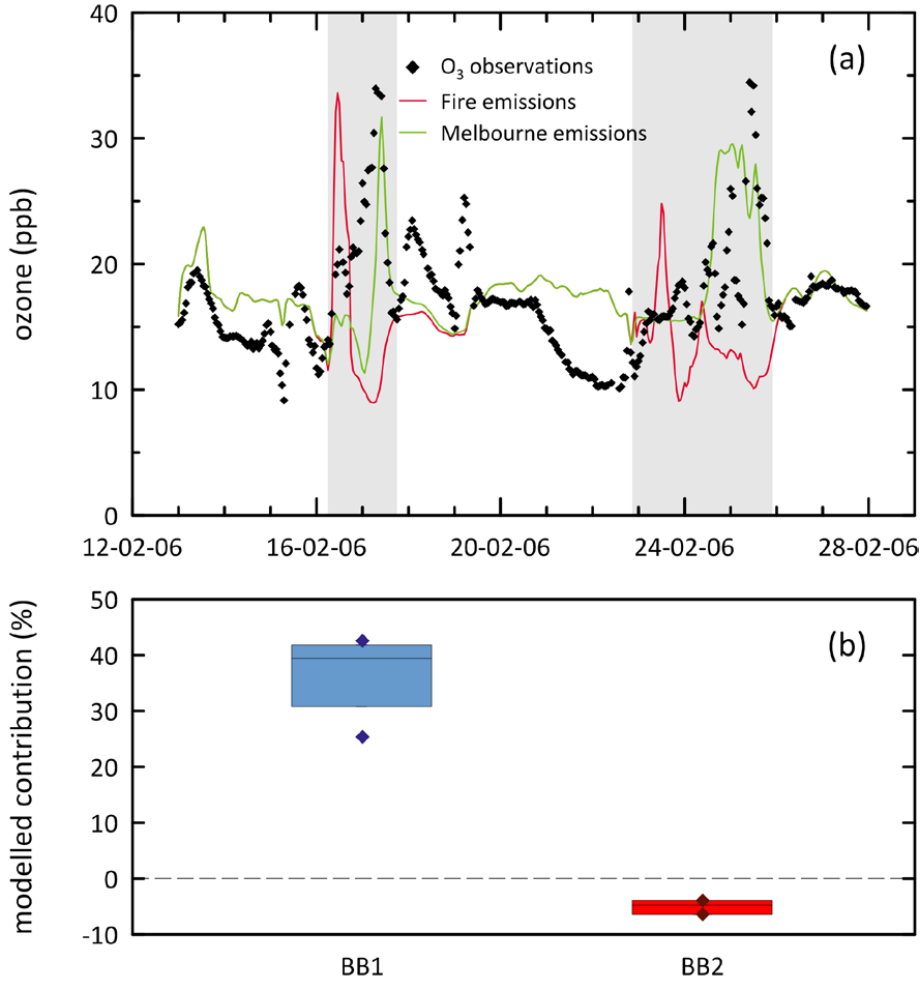

Figure 8 a) Simulated contribution to O_3 formation at Cape Grim from Robbins Island fire emissions (red line) and Melbourne emissions (green line). Observations are black symbols. The periods corresponding to BB1 and BB2 are shaded; b) simulated contribution of the fire to excess O_3 for BB1 and BB2 at all 5 grid points surrounding Cape Grim, where upper and lower diamonds are minimum and maximum contribution.

Atmos. Chem. Phys. Discuss., doi:10.5194/acp-2016-932, 2016
Manuscript under review for journal Atmos. Chem. Phys.
Published: 5 December 2016

Atmospheric Chemistry and Physics Discussions

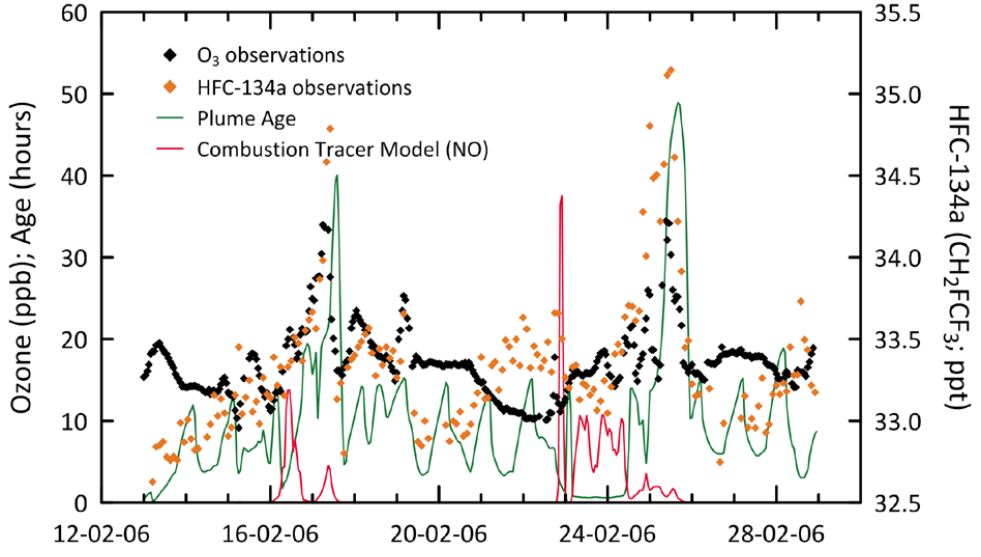

Figure 9. Simulated plume age (green line), simulated combustion tracer (NO) (red line), observed O_3 (black symbols) and HFC-134a (orange symbols) over the 2 week duration of the fire.